Environ Chem Lett (2010) 8:79–85
DOI 10.1007/s10311-008-0195-5

ORIGINAL PAPER

Influence of support on catalytic behavior of nickel catalysts in the steam reforming of ethanol for hydrogen production

Humberto V. Fajardo · Elson Longo · Daniela Z. Mezalira · Giselle B. Nuernberg · Gizelle I. Almerindo · André Collasiol · Luiz F. D. Probst · Irene T. S. Garcia · Neftalí L. V. Carreño

Received: 3 July 2008 / Accepted: 25 November 2008 / Published online: 18 December 2008

Abstract Al_2O_3, MgO, SiO_2 and ZnO-supported nickel catalysts were prepared and evaluated in the ethanol steam reforming for hydrogen production. It is shown that the catalytic behavior can be influenced depending on the experimental conditions employed and chemical composition of the catalyst.

Keywords Steam reforming · Ethanol · Hydrogen · Nickel catalysts

Introduction

Hydrogen is, at present, mainly used as raw material for the chemical and refining industries. However, in the near future, hydrogen will play an important role in the energy sector. In combination with fuel cells, has been proposed as a major energy source which could contribute to the reduction of atmospheric pollution and greenhouse gases emissions, and reduction of global dependency on fossil fuels. The main process for hydrogen production includes steam reforming of natural gas, which is based on a fossil resource and is always associated with the emissions of local pollutants. Therefore, due to the expected increasing demand for energy together with environmental concerns related to reducing atmospheric pollution, the development of alternative methods for hydrogen production, especially from renewable sources, has attracting much attention (de Bruijn 2005; Armor 2005). An alternative and promising way to produce hydrogen is to use ethanol as the feedstock for the steam reforming process. This alcohol has several advantages compared to fossil fuels but the most important is probably its renewable origin. It can be easily obtained from several biomass sources, including through the fermentation of sugarcane. The bio-ethanol-to-hydrogen system has the positive feature of being CO_2 neutral, thus environmental friendly, since the CO_2 produced is consumed for biomass growth and a nearly closed carbon cycle results. In previous studies, several catalysts have been proposed to be further considered for practical applications in ethanol steam reforming. Nobel metal-based catalysts frequently exhibit better activity when compared to non-noble metal catalysts, however, these catalysts are very expensive. On the other hand, Ni-based catalysts have shown high activity and selectivity, moreover, they are cheap (Haryanto et al. 2005; Vaidya and Rodrigues 2006; Ni et al. 2007). In this study, a comparison between Al_2O_3, MgO, SiO_2 and ZnO-supported nickel catalysts in the ethanol steam reforming to produce hydrogen is reported.

H. V. Fajardo (✉)
Departamento de Química,
Universidade Federal de Ouro Preto,
Ouro Preto, MG 35400-000, Brazil
e-mail: hfajardoufsc@hotmail.com; hfajardo@iceb.ufop.br

E. Longo
Departamento de Bioquímica e Tecnologia Química,
Universidade Estadual Paulista, Araraquara,
SP 15385-000, Brazil

D. Z. Mezalira · G. B. Nuernberg · G. I. Almerindo · A. Collasiol · L. F. D. Probst
Departamento de Química,
Universidade Federal de Santa Catarina,
Florianópolis, SC 88040-900, Brazil

I. T. S. Garcia · N. L. V. Carreño
Departamento de Química Analítica e Inorgânica,
Universidade Federal de Pelotas, Capão do Leão,
RS 96010-900, Brazil

Experimental

Catalyst preparation

The Ni catalysts were prepared by wet impregnation method, using nickel nitrate [$Ni(NO_3)_2{\cdot}6H_2O$—Fluka, 99.9%] as the metal precursor. A known amount of the nickel salt was dissolved in water and the commercial Al_2O_3 (Riedel-de Haën), MgO (Riedel-de Haën), SiO_2 (Vetec) and ZnO (Vetec) oxides were added to its respective solution under continuous stirring. The slurries were heated slowly to 90°C and maintained at that temperature until nearly all the water evaporated. The solid residues were dried at 120°C for 12 h and then calcined in air atmosphere at a temperature of 700°C for 2 h.

Catalyst characterization

Samples were characterized by N_2 physisorption isotherms (Autosorb-1C—Quantachrome). Specific surface areas were calculated according to the Brunauer–Emmett–Teller (BET) method, and the pore size distributions were obtained according to the Barret–Joyner–Halenda (BJH) method. For the determination of the Ni content an atomic spectrometer (Varian Model SpectrAA 50), equipped with an air–acetylene flame atomizer and a Hitachi hollow cathode lamp (HLA 4S) was used. Temperature programmed reduction analyses (TPR) were performed in a quartz reactor under 5 vol% H_2/N_2 flow (30 mL min^{-1}) from 30 to 920°C at a heating rate of 5°C/min. A thermal conductivity detector was used to follow the H_2 consumption. The crystalline phases were characterized by X-ray diffraction (XRD) in a Siemens D-5000.

Catalytic testing

Catalytic performance tests were conducted at atmospheric pressure with a quartz fixed-bed reactor fitted in a programmable oven, in the temperatures of 400 and 550°C. The catalyst was previously reduced in situ under hydrogen atmosphere at 600°C for 2 h. The water:ethanol mixture (molar ratio 3:1) was pumped into a heated chamber and vaporized. The water–ethanol gas (N_2) stream (30 mL min^{-1}) is then fed to the reactor containing 100 mg of the catalyst. The reactants and the composition of the reactor effluent were analyzed with a gas chromatograph (Shimadzu GC 8A), equipped with a thermal conductivity detector, Porapak-Q and a 5A molecular sieve column. Catalyst activity was evaluated in terms of ethanol conversion. We defined ethanol conversion as:

$$\mathrm{CEtOH}(\%) = (\mathrm{Qconv}/\mathrm{QEtOH}) \times 100 \quad (1)$$

Here, Qconv represents the quantity (moles) of converted ethanol; QEtOH represents the total quantity (moles) of ethanol feed into the reactor.

We defined the catalyst selectivity as the mole fraction of each product as:

$$\mathrm{SP}(\%) = (\mathrm{QP}/\mathrm{QsP}) \times 100 \quad (2)$$

Here, QP represents the number of moles of each product; QsP represents the sum of the moles of the products, but the moles of solid products (such as small amount of coke) are not included.

Results and discussion

Catalysts characterization

The chemical analysis and specific surface area values of all the nickel-based catalysts are summarized in Table 1. The specific surface area ranged from 15 to 190 $m^2\ g^{-1}$. The Ni/SiO_2 sample presented the highest specific surface area, 190 $m^2\ g^{-1}$.

With the aim of identifying the phases present in the catalytic samples, XRD and TPR analysis were carried out. Figure 1 shows the XRD patterns of the fresh nickel-supported catalysts. The NiO phase presence in the fresh catalysts suggests the decomposition of nickel nitrate in air at the calcination temperature to form the NiO species during the preparation of catalysts. The XRD profile of the Ni/SiO_2 catalyst presents a broad peak at 22° assigned to amorphous silica. According to the literature, the reflection peaks at $2\theta = 37.28$, 43.3, 62.8, and 75.3° can be attributed due to the NiO phase, however the reflection peaks at $2\theta = 37.28$ and 62.8° can also be assigned to nickel silicate (Takahashi et al. 2005). The diffraction peaks of the Ni/Al_2O_3 sample can be assigned to major three oxides, NiO, $NiAl_2O_4$ and γ-Al_2O_3. It is well known that NiO react easily with γ-Al_2O_3 to form surface or bulk $NiAl_2O_4$ spinel. Due to the peak broadening and superimposition of γ-Al_2O_3 and $NiAl_2O_4$ phases, it was difficult to clearly distinguish γ-Al_2O_3 and $NiAl_2O_4$ phases by means of XRD.

Table 1 Chemical (Ni %wt) and N_2 physisorption analyses of the nickel-based catalysts

Catalysts	S_{BET} (m^2/g)	V_{BJH} (cm^3/g)	Ni (%)
Ni/Al_2O_3	164	0.462	17.4
Ni/MgO	18	0.487	8
Ni/SiO_2	190	0.290	11.9
Ni/ZnO	15	0.012	11.8

S_{BET} specific surface area, V_{BJH} pore volume

However, the formation of $NiAl_2O_4$ in Ni/Al_2O_3 could be justified by temperature programmed reduction analyses (Valentini et al. 2003). The X-ray diffractogram recorded for the Ni/ZnO catalyst shows the wurtzite structure of ZnO and the presence of the NiO phase, indicated by peaks at 37.2 and 43.28° (Cong et al. 2006). The XRD profile of the Ni/MgO catalyst presents peaks at 37, 43, 62.4 and 66° for 2θ which are ascribed to MgO and $MgNiO_2$ phases (Furusawa and Tsutsumi 2005).

The determination of reducible species at the surface of the catalyst and the temperature at which these species are reduced, gives important information on catalysis. The TPR profiles of the nickel-based catalysts are shown in Fig. 2. TPR spectrum of Ni/Al_2O_3 catalyst shows a maximum H_2 consumption peak at around 820°C, which can be assigned to the reduction of $NiAl_2O_4$ spinel structure, indicating a high metal-support interaction, promoted by the calcination temperature applied to the material (Fajardo et al. 2005). The Ni/SiO_2 catalyst presents two reduction peaks with maximums at 450 and 610°C. The first of them is found in the zone assigned by literature to NiO species of low interaction with the support, whereas the signal at 610°C is attributed to a nickel oxide interacting chemically with the support as cited by some authors, it can ascribed to the formation of nickel silicate (Pompeo et al. 2005). The Ni/ZnO catalyst presents two reduction peaks with maximums at 480 and 620°C. The former can be assigned to the reduction of bulk NiO in weak interaction with ZnO surface, while the peak at around 620°C can be attributed to the reduction of Ni ions that interacted strongly with the zinc oxide support (Yang et al. 2006). In the case of Ni/MgO catalyst, three reduction peaks at around 325, 600 and 775°C were observed. It is suggested that the peak at around 325°C should be assigned to the reduction of NiO located on the MgO surface or to the reduction of some form of Ni^{2+} ions having square-pyramidal coordination in the outermost layer of the catalyst structure, while the reduction peak at 600°C should be assigned to the reduction of NiO located in the bulk. The reduction peak at around 775°C can be assigned to Ni^{2+} ions in the NiO–MgO ($MgNiO_2$) solid solution lattice (Furusawa and Tsutsumi 2005).

Catalytic tests

The influence of operating temperature on the ethanol conversion and product selectivities from the ethanol steam reforming over nickel-based catalysts was studied. The catalytic behaviors of the different catalysts were also studied and compared. The ethanol steam reform reaction can be accompanied by a series of parallel reactions (secondary compared the steam reform) such as, dehydration, dehydrogenation and decomposition reactions. These reactions are more or less promoted depending on the nature of the catalyst, the type of interaction with the surface of the solid material and the different reaction

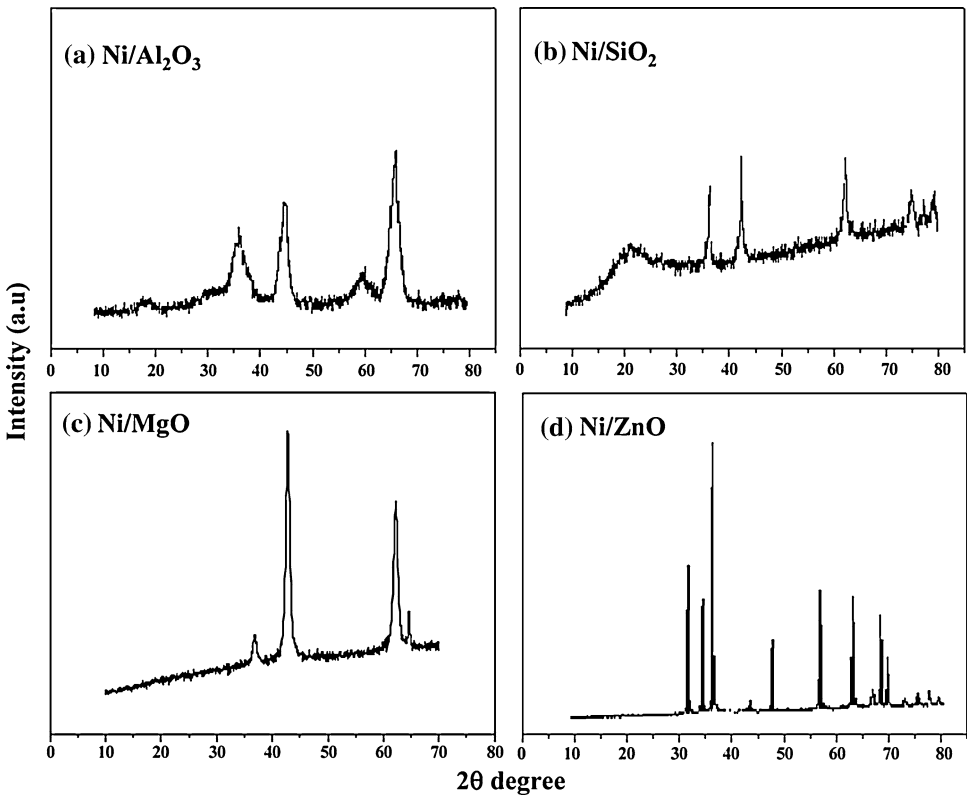

Fig. 1 X-ray diffraction patterns for the different nickel-based catalysts

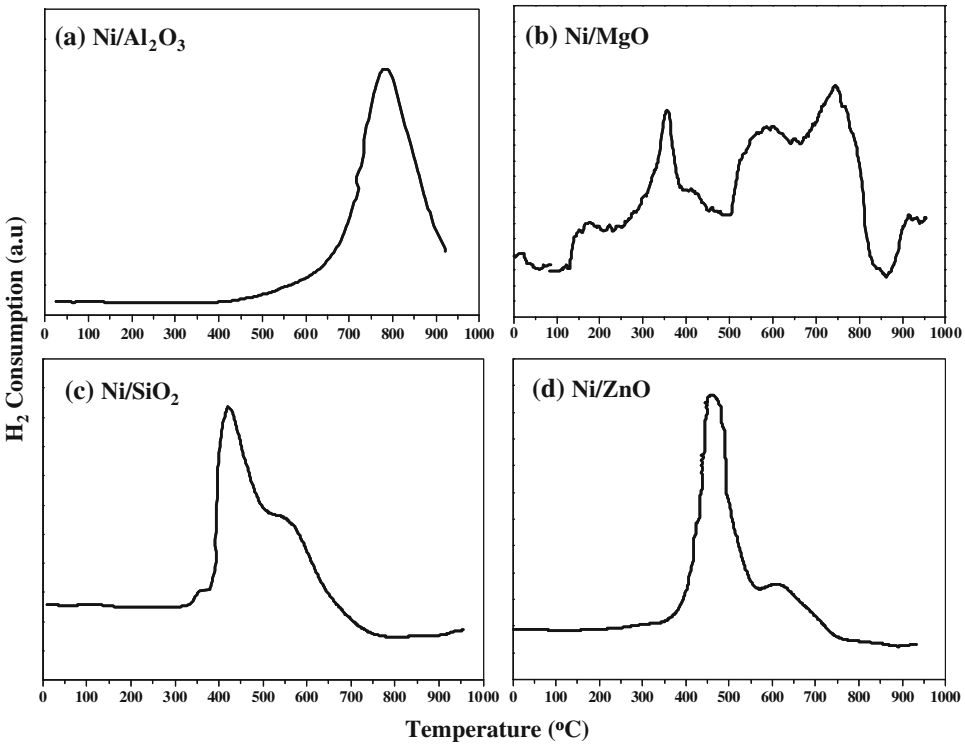

Fig. 2 Temperature programmed reduction profiles for the different nickel-based catalysts

conditions (Haryanto et al. 2005; Vaidya and Rodrigues 2006; Ni et al. 2007). It was observed (Fig. 3a) that the steam reforming reaction of ethanol (Eq. 3) is negligible, over Ni/Al_2O_3 catalyst at temperature of 400°C.

$$C_2H_5OH + 3H_2O \rightarrow 2CO_2 + 6H_2 \quad (3)$$

Instead, dehydration of ethanol (Eq. 4), which occurs to an appreciable extent producing ethylene, and an ethanol decomposition reaction (Eq. 5) seem to occur as the main reactions.

$$C_2H_5OH \rightarrow C_2H_4 + H_2O \quad (4)$$

$$C_2H_5OH \rightarrow 2C + 2H_2 + H_2O \quad (5)$$

This result is consistent with the characteristics of the support (Al_2O_3) that possess acidic sites that are required for the dehydration route (Haryanto et al. 2005; Vaidya and Rodrigues 2006; Ni et al. 2007). In addition, according to TPR results, the $NiAl_2O_4$ phase presence is great for this sample, indicating a great metal-support interaction. In that way, the active phase (Ni) would be less accessible and the support would be the main responsible for the catalytic activity in this temperature. The conversion of ethanol reached 35% at the beginning of the test. However, the ethanol conversion decreased from 35 to 25% after 250 min in time on stream with very little difference in the product distribution. The coke formation from decomposition reaction of ethanol and ethylene polymerization (Eq. 6) may be considered as the main reason for the catalyst deactivation observed in this case. Since ethylene is a precursor of coke formation, and may lead to catalyst deactivation, its presence is highly undesirable.

$$C_2H_4 \rightarrow \text{coke} \quad (6)$$

When the temperature increased to 550°C (Fig. 3b) the conversion of ethanol reached 100%, remaining stable until the end of the run. The temperature increase produces a drop in ethylene selectivity and an increase in hydrogen selectivity. From the analysis of product distribution obtained at 550°C, it can be observed that hydrogen selectivity is approximately three times higher than carbon dioxide selectivity, suggesting that ethanol steam reforming (Eq. 3), instead ethanol decomposition (Eq. 5), was promoted. However, the presence of ethylene in the product stream of Ni/Al_2O_3 catalyst is still high indicating that ethanol dehydration is the main reaction involved.

Interestingly, over Ni/MgO at 400°C of reaction temperature, the dehydration of ethanol to ethylene was the most important reaction with selectivity to C_2H_4 of approximately 70% (Fig. 3c). Over this catalyst ethanol decomposition to H_2, C and H_2O also takes place to a large extent. The acetaldehyde formation, from ethanol dehydrogenation (Eq. 7), which would be expected due to basic properties of the support (MgO), was not observed at this temperature.

$$C_2H_5OH \rightarrow CH_3CHO + H_2 \quad (7)$$

It is well known that the basic and acidic properties of the supports oxides are essential parameters directly affecting the primary selectivity for acetaldehyde or ethylene. Basic

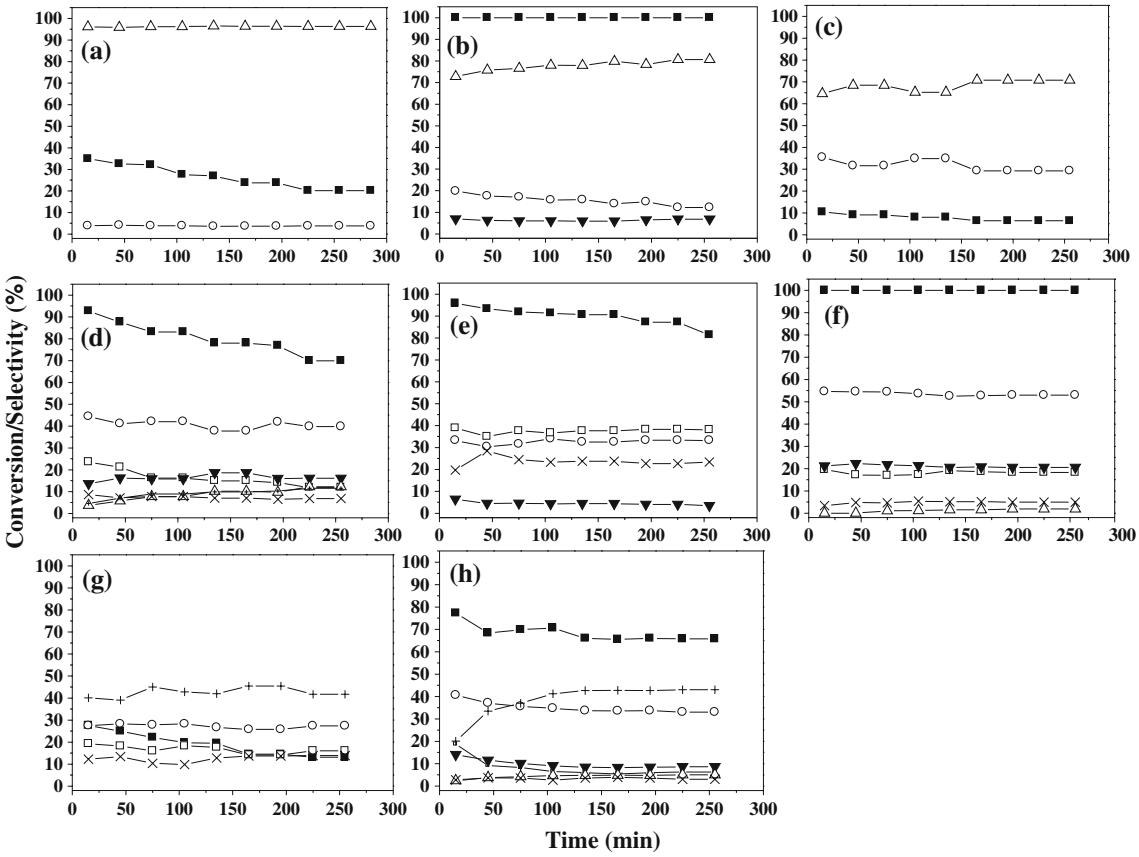

Fig. 3 Steam reforming of ethanol over different nickel-based catalysts. *Filled square* C_2H_5OH conversion, *open circle* H_2, *open triangle* C_2H_4, *filled triangle* CO_2, *open square* CH_4, *plus symbol* CH_3CHO; *multiplication symbol* CO, selectivities

sites are predominant in the ethanol dehydrogenation to acetaldehyde, whereas ethylene would be produced with an essential role of the acidic sites of the support. However, in spite of alcohol dehydration be much faster over acidic oxides than over basic oxides, alcohol dehydration into alkenes could be catalyzed by the support over pairs of acidic and basic sites. Ethylene formation from ethanol could occur via a mechanism involving both a weak Lewis acidic site and a strong Bronsted basic site (Sánchez-Sánchez et al. 2007; Di Cosimo et al. 1998; Liguras et al. 2003). Similar results were reported by Liguras et al. (2003), where the selectivity toward C_2H_4 over Ru/Al_2O_3 was similar to that over Ru/MgO. The results points out that the acidity of catalysts, in spite that is an important factor in the formation of ethylene, was not the only catalyst functionality that influences on the observed ethylene production and, as indicated by the authors, the different reforming activity associated with the metal phases may explain the selectivity toward ethylene independently of the acidity of the supports, taking into account that ethylene can be reformed under certain reaction conditions. In addition, according to Di Cosimo et al. (1998), pure MgO was poorly active in acetaldehyde production from ethanol, however, small amounts of aluminum ions added to MgO were sufficient to make the catalyst very active in ethanol dehydrogenation to acetaldehyde. When the temperature increased to 550°C (Fig. 3d), it was observed an increase in the ethanol conversion, reaching 95% at the beginning of the test. The main compounds detected at this temperature were H_2, CH_4, CO_2, CO, C_2H_4 and CH_3CHO. The product distribution indicates that at this stage the ethanol steam reforming (Eq. 3) and decomposition to H_2, CH_4 and CO (Eq. 8) predominated, meanwhile ethanol dehydrogenation and dehydration were also involved. The occurrence of the water gas shift reaction (Eq. 9) can not be ruled out. It is of interest to note that the production of ethylene, which is an undesirable product, is significantly suppressed with increasing reaction temperature, suggesting that ethylene steam reforming (Eq. 10) is promoted due to the excess of water in the system.

$$C_2H_5OH \rightarrow CH_4 + CO + H_2 \quad (8)$$

$$CO + H_2O \rightarrow CO_2 + H_2 \quad (9)$$

$$C_2H_4 + 2H_2O \rightarrow CH_4 + CO_2 + 2H_2 \quad (10)$$

Over Ni/SiO_2 catalyst at 400°C of reaction temperature (Fig. 3e), the ethanol conversion reached 95% at the

beginning of the test. The reaction products were almost exclusively H_2, CO and CH_4, with lower amounts of CO_2. This seems to indicate that the decomposition reaction of ethanol (Eq. 8) is clearly favored. The low selectivity to CO_2 could be produced either by the water gas shift reaction or by the ethanol steam reforming. When the temperature increased to 550°C (Fig. 3f), the conversion of ethanol reached the maximum, remaining stable until the end of the test. The selectivities of H_2 and CO_2 increased to 55 and 22%, respectively, while the selectivities of CH_4 and CO decreased to 16 and 4%, respectively, indicating the effect of increasing the extents of the water gas shift reaction and methane steam reforming reaction (Eq. 11). A small amount of C_2H_4 was also detected with a selectivity of 1%.

$$CH_4 + H_2O \rightarrow CO + 3H_2 \quad (11)$$

Ethanol conversion over Ni/ZnO catalyst at 400°C of reaction temperature was less than 30% (Fig. 3g). The main products besides acetaldehyde were hydrogen, carbon monoxide and methane, indicating that ethanol dehydrogenation and decomposition reactions were promoted. Increasing reaction temperature results in an increase of the conversion of ethanol (Fig. 3h), a decrease of the selectivity toward CO and CH_4 and an increase of the selectivity toward CO_2. This behavior may be attributed to the ethanol steam reforming (Eq. 3), methane steam reforming and water gas shift reaction, which become predominant under this condition. The selectivity toward acetaldehyde did not change very much, suggesting that ethanol dehydrogenation remains as the one of the main reactions involved. It is interesting to observe that ethylene is detected under this condition indicating that dehydration of ethanol is taking place.

Conclusions

The experimental results indicated that the reaction conditions and the nature of nickel-based catalysts influenced the ethanol steam reforming process. The supports played an important role, acting on the ethanol conversion and on the product selectivities. When we compare the conversion of ethanol and selectivity to hydrogen over nickel-based catalysts, at a reaction temperature of 400°C, it can be seen that the activity was: $Ni/SiO_2 \gg Ni/Al_2O_3 > Ni/ZnO > Ni/MgO$.The highest conversion over Ni/SiO_2, could indicate that there is a greater quantity of active sites available for this catalyst. Probably, the high surface area of silica allows a greater dispersion of the metal active phase. However, selectivity to hydrogen was affected by the support used and occurred in the following order: $Ni/SiO_2 \approx Ni/MgO > Ni/ZnO \gg Ni/Al_2O_3$.The low H_2 selectivity presented by Ni/Al_2O_3 could be due to the great C_2H_4 formation promoted by this catalyst. In addition, according to the results, it is possible to conclude that at 400°C only Ni/SiO_2 was active for ethanol steam reforming and at 500°C of reaction temperature, Ni/SiO_2 and Ni/MgO showed activity for ethanol steam reforming.

Acknowledgments This research was supported by the Brazilian funding support agencies: CNPq and FINEP.

References

Armor JN (2005) Catalysis and the hydrogen economy. Catal Lett 101:131–135. doi:10.1007/s10562-005-4877-3

Cong CJ, Hong JH, Liu QY, Liao L, Zhang KL (2006) Synthesis, structure and ferromagnetic properties of Ni-doped ZnO nanoparticles. Solid State Commun 138:511–515. doi:10.1016/j.ssc.2006.04.020

de Bruijn F (2005) The current status of fuel cell technology for mobile and stationary applications. Green Chem 7:132–150. doi:10.1039/b415317k

Di Cosimo JI, Díez VK, Xu M, Iglesia E, Apesteguía CR (1998) Structure and surface and catalytic properties of Mg–Al basic oxides. J Catal 178:499–510. doi:10.1006/jcat.1998.2161

Fajardo HV, Martins AO, Almeida RM, Noda LK, Probst LFD, Carreño NLV, Valentini A (2005) Synthesis of mesoporous Al_2O_3 macrospheres using the biopolymer chitosan as a template: a novel active catalyst system for CO_2 reforming of methane. Mater Lett 59:3963–3967. doi:10.1016/j.matlet.2005.07.071

Furusawa T, Tsutsumi A (2005) Comparison of Co/MgO and Ni/MgO catalysts for the steam reforming of naphthalene as a model compound of tar derived from biomass gasification. Appl Catal A 278:207–212. doi:10.1016/j.apcata.2004.09.035

Haryanto A, Fernando S, Murali N, Adhikari S (2005) Current status of hydrogen production techniques by steam reforming of ethanol: a review. Energy Fuels 19:2098–2106. doi:10.1021/ef0500538

Liguras DK, Kondarides DI, Verykios XE (2003) Production of hydrogen for fuel cells by steam reforming of ethanol over supported noble metal catalysts. Appl Catal B 43:345–354. doi:10.1016/S0926-3373(02)00327-2

Ni M, Leung DYC, Leung MKH (2007) A review on reforming bio-ethanol for hydrogen production. Int J Hydrogen Energy 32:3238–3247. doi:10.1016/j.ijhydene.2007.04.038

Pompeo F, Nichio NN, González MG, Montes M (2005) Characterization of Ni/SiO_2 and $Ni/Li\text{-}SiO_2$ catalysts for methane dry reforming. Catal Today 107–108:856–862. doi:10.1016/j.cattod.2005.07.024

Sánchez-Sánchez MC, Navarro RM, Fierro JLG (2007) Ethanol steam reforming over $Ni/MxOy\text{-}Al_2O_3$ (M = Ce, La, Zr and Mg) catalysts: Influence of support on the hydrogen production. Int J Hydrogen Energy 32:1462–1471. doi:10.1016/j.ijhydene.2006.10.025

Takahashi R, Sato S, Sodesawa T, Tomiyama S (2005) CO_2-reforming of methane over Ni/SiO_2 catalyst prepared by homogeneous precipitation in sol-gel-derived silica gel. Appl Catal A 286:142–147

Vaidya PD, Rodrigues AE (2006) Insight into steam reforming of ethanol to produce hydrogen for fuel cells. Chem Eng J 117:39–49. doi:10.1016/j.cej.2005.12.008

Valentini A, Carreño NLV, Probst LFD, Lisboa-Filho PN, Schreiner WH, Leite ER, Longo E (2003) Role of vanadium in Ni:Al_2O_3 catalysts for carbon dioxide reforming of methane. Appl Catal A 255:211–220. doi:10.1016/S0926-860X(03)00560-X

Yang Y, Ma J, Wu F (2006) Production of hydrogen by steam reforming of ethanol over a Ni/ZnO catalyst. Int J Hydrogen Energy 31:877–882. doi:10.1016/j.ijhydene.2005.06.029